Iğdır Üniversitesi Fen Bilimleri Enstitüsü Dergisi, 12(4): 2166 - 2174, 2022
Journal of the Institute of Science and Technology, 12(4): 2166 - 2174, 2022
ISSN: 2146-0574, eISSN: 2536-4618

Physics **DOI: 10.21597/jist.1129531**

Research Article

Received: 11.06.2022 **Accepted: 16.08.2022**

To Cite: Bulut P, 2022. Effects of Van der Waals Interaction and Hubbard Term Correction on First Principles Calculations of Structural and Lattice Dynamical Properties of AgCl. Journal of the Institute of Science and Technology, 12(4): 2166 - 2174.

Effects of Van der Waals Interaction and Hubbard Term Correction on First Principles Calculations of Structural and Lattice Dynamical Properties of AgCl

Pınar BULUT

ABSTRACT: Structural, dielectric, and lattice dynamical properties of AgCl in the rock-salt structure are studied using density functional theory within generalized gradient approximation(GGA) in Perdew-Burke-Erzhenhof(PBE) parametrization and plane-wave pseudopotential method. The effect of van der Waals interaction (vdW) and Hubbard-U is investigated in detail for the lattice parameters, bulk modulus, dielectric, and phonon properties and compared to available experimental measurements. It is found that, inclusion of vdW interactions together with Hubbard U parameter to the standard GGA-PBE (PBE+vdW+U) improved the agreement with experimental lattice constant and bulk modulus of rock-salt AgCl. Moreover, PBE+vdW+U method is also correctly describes the acoustic and transverse optical (TO) phonon dispersion relation curves. The large underestimation (15%) of GGA-PBE in the longitudinal optical (LO) modes with respect to experiment is also decreased to 5% within the PBE+vdW+U method. This work demonstrates the applicability and accuracy of the van der Waals interaction and Hubbard-U term in predicting the structural, dielectric, and lattice dynamical properties of AgCl in the rock-salt structure.

Keywords: Halide semiconductors, density functional theory, phonon dispersion

Pınar BULUT (**Orcid ID:** 0000-0001-5818-2263), Namık Kemal University, Faculty of Arts and Sciences, Department of Physics, Tekirdağ, Türkiye

Corresponding Author: Pınar BULUT, e-mail: pbulut@nku.edu.tr

INTRODUCTION

Group I-VII halide semiconductors have received much attention for experimental and theoretical studies during the past decades for their interesting optical and electronic properties (Grundmann et al., 2013; Ahn and Park, 2016). Cuprous and silver halides are wide-gap and direct band gap semiconductors used in various applications in optoelectronic devices. They have a variety of polymorphs at varying temperature and pressure ranges (Faustino et al., 2018; Li et al., 2008; Mellander et al., 1981). Moreover, sphalerite phase of silver iodide is worth to consider, it crystallizes in both cubic zincblende and hexagonal wurtzite structure at the same time under normal conditions (Patnaik and Sunandana, 1998; Mellander, 1982). Cuprous and silver halides are also exhibit very low thermal conductivity which is important for many applications such as thermoelectricity (Faustino et al., 2018; Mukhopadhyay et al., 2017; Yang et al., 2017). In addition, cuprous halides are well known materials due to their transparent p-type behaviour and that is less common simultaneous conductivity and transparency in a p-type material.

In particular, CuCl has been actively studied for its unusual linear and nonlinear optical properties (Saito et al., 1995; Masumoto et al., 1989). Recently CuI has been identified as a native p-type transparent thermoelectric material and employed in solar cells (Grundmann et al., 2013; Faustino et al., 2018; Yang et al., 2017). CuBr has been proposed as an alternative inorganic p-type semiconductor. Due to its high transparency, CuBr thin films are promising hole-transport materials for applications in diverse optoelectronic devices such as thin film transistors and solar cells (Zhu et al., 2019).

Silver halides are valued for their high photosensitivity so they are used as the main components of photographic process (Cha and Jung, 2017). For instance AgI is the first photographic material designed by Becquerel (Grundmann et al., 2013; Becquerel, 1839; Zhang and Jiang, 2019). AgI is also used for weather modifications like rain seeding (Cha and Jung, 2017). Silver halides are very good electrolytes because of their high ionic conductivity (Li et al., 2008; Wang et al., 2003). Another special role is attributed to silver halides which is that they act as liquid semiconductors (Kirchhoff et al., 1994) and they are a promising candidate for photocatalysis (An et al., 2016). In Silver halides, Ag atom has completely filled 4*d* shell and a single 5*s* electron which can be transferred to the halide atom. This leads to strong hybridization of the silver *d* states and the halide *p* states which causes a considerable complexity in the electronic structure (Vogel et al., 1998; Tejeda et al., 1975; Smith, 1976; Tejeda et al., 1974) and separates silver halides from other compounds.

To date, for silver halides the theoretical and experimental studies are generally focused on the electronic structure properties, ionic transport properties, and optical absorption. (Okoye, 2004; Nunes et al., 1998; Zhang and Jiang, 2019; Benmessabih et al., 2007; Gao et al., 2018; Palomino-Rojas et al., 2008; Victora, 1997; Amrani et al., 2008). Recently, (Assis et al., 2020) report the synthesis of Ag nanoparticle/AgX (X=Cl, Br and I) composites by electron beam irradiation and presented the Raman spectra and they also calculated the some structural properties of silver halides. However, this experimentally and theoretically detailed study does not concentrate on examining phonon distributions. Some early works include the investigation of the phonon properties. Li *et. al.* (Li et al., 2008) calculated the phonon instabilities of AgI under pressure. Li *et. al.* (Li et al., 2006) calculated the phonon frequencies of AgCl and AgBr within GGA but they used the experimental lattice constants. (Yang et al., 2019) is used GGA-PBE functionals for the calculation of phonon dispersion of AgCl and AgBr but the softening of the calculated transverse acoustic Γ-L branch is not supported by the experimental measurement.

In the recent studies, the long range van der Waals interactions for the nonlocal electron correlation effects are found to be important not only for organic or layer compounds but also for metals, semiconductors, and ionic compounds (Klimes et al., 2010; Zhang et al., 2011). But, as far as we know, in previous studies there is no study in which both Hubbard U term and van der Waals interaction effects are taken into account to first principle phonon calculations for AgCl. In this study, we have studied structural, dielectric, and, vibrational properties of rock-salt AgCl from first principles. Inclusion of Hubbard U term and/or van der Waals interactions are also investigated and discussed. The organization of this paper is as follows: we present the computational details in Sec. 2. In Sec. 3, we discuss the structural, dielectric and phonon properties. And finally in Sec. 4 we give the conclusion.

MATERIALS AND METHODS

First principle calculations on structural, dielectric and lattice dynamical properties of AgCl was performed using density functional theory (DFT) within the Quantum Espresso code (Giannozzi et al., 2009; Giannozzi et. al., 2017). Quantum Espresso (QE) is a multipurpose software code for ab-initio calculations of condensed matter systems and are ideally suited for structural optimizations, ground state calculations, linear response calculations and ab initio molecular dynamics. Quantum Espresso code is based on density functional theory, plane wave basis sets, and pseudopotentials. The Perdew-Burke-Ernzerhof (PBE) parametrization of generalized gradient approximation (GGA) was selected for the exchange correlation energy (Perdew et al., 1996). PBE is the most popular GGA functional and it is a non-empirical functional with beter accuracy for wide range of systems.

During the calculations, the interaction between the valence electron and the ionic core was described by ultrasoft pseudopotentials (Vanderbilt, 1990) for a plane wave basis set of wavefunctions. The converged kinetic energy cut-off was obtained as 80 Ry and a $8\times8\times8$ Γ centered Monkhorst-Pack k-grid was used for geometric optimization. Smearing with degauss has been set at 0.25 and convergence threshold on forces for ionic minimization was at 10^{-12}. Charge density cut-off 640 Ry was found to be converged for calculations. Born effective charges (Z^*), dielectric constants and phonon properties were calculated within density functional perturbation theory (DFPT) (Baroni et al., 2001) as implemented in Quantum Espresso code. A $4\times4\times4$ q-grid was found to be well converged for phonon calculations.

Hubbard U term (PBE+U) is only a correction to traditional density functional theory and account for the over-hybridization and localization of electron orbitals (Anisimov et al., 1991). Assuming that implementing a Hubbard U term to the PBE (PBE+U) (Anisimov et al., 1991) have a significant effect on strongly correlated *d* or *f* electron (Zhang and Jiang, 2019; Jiang, 2018; Jossou et al., 2017; Consiglio and Tian, 2016; Tolba et al., 2018), calculations were performed with and without U term. For PBE+U calculations, following (Gao et al., 2018), U_{eff} =U-J=5 eV value was applied to the d orbitals of Ag.

In addition, due to van der Waals interactions have considered to be important for structural and phonon properties, optB88- vdW functional of Klimes *et al.* (Klimes et al., 2010) was added to the PBE functional (PBE+vdW). OptB88vdw (PBE+vdw) is a non-local correlation functional that approximately accounts for long range interactions (Choudhary et al., 2018; Klimes et al., 2010).

Calculations were performed with and without or both U term and van der Waals interaction (PBE, PBE +U, PBE +vdW, PBE +U+vdW).

RESULTS AND DISCUSSION

Structural and dielectric properties

Table 1. Lattice constant a_0 (in A^0), bulk modulus B_0 (in GPa), pressure derivative of bulk modulus B'

Study	a_0 (Å)	B_0 (GPa)	B'
This Work (PBE)	5.612(1.2%)	42.19(10%)	5.30
This Work (PBE + U)	5.650(1.9%)	40.41(14%)	5.27
This Work (PBE + vdW)	5.566(0.36%)	49.27(5%)	5.19
This Work (PBE + U+vdW)	5.559**(0.23%)**	47.46**(1%)**	5.17
Other Calc (GGA) (Okoye, 2004)	5.61(1.2%)	43.37(%7.7)	5.65
Other Calc (LDA) (Nunes et al., 1998)	5.41(2.5%)	66.8(20%)	5.20
Expt.(Hull and Keen, 1999)	5.546	47	4

AgCl crystallize under normal conditions in the rock-salt (NaCl) structure in space group $Fm\bar{3}m$ (225) below its melting point (728 K) and has a face centered cubic structure. Rock- salt structure AgCl crystal contains two atoms per primitive cell. Ag atom is located at 4*a* (0,0,0) and Cl atom is in 4*b* (1/2,1/2,1/2) Wyckoff positions. Calculated structural properties are given in Table 1 along with available experimental results and other calculations. Bulk modulus and its pressure derivative are obtained by fitting the Birch-Murnaghan equation of state (EOS) (Hebbache and Zemzemi, 2004).

$$E(V) = E_0 + \frac{9V_0B_0}{16}\left\{\left[\left(\frac{V_0}{V}\right)^{\frac{2}{3}} - 1\right]^3 B_0' + \left[\left(\frac{V_0}{V}\right)^{\frac{2}{3}} - 1\right]^2 \left[6 - 4\left(\frac{V_0}{V}\right)^{\frac{2}{3}}\right]\right\} \quad (1)$$

where, $B_0$is the bulk modulus, B_0' is the pressure derivative of the bulk modulus, V_0 is the equilibrium volume of the crystalline, E_0 is the total energy of crystalline unit cell at this volume. Our calculated lattice parameters and bulk modulus are almost the same with other GGA calculations [13]. While applying Hubbard U term to Ag *d* states (PBE+U) doesn't improve the results, optimizations with van der Waals interaction (PBE+vdW) predict more accurate values compared to PBE. The best agreement to experimental values for lattice constant, bulk modulus and pressure derivative of bulk modulus is obtained by the calculations with both Hubbard U parameter and van der Waals functional (PBE+U+vdW). Local-density approximation (LDA) calculations give much larger values (Nunes et al., 1998). PBE overestimates the lattice constant from experiment about 1.2% and bulk modulus about 10%. This overestimation is typical from the implementation of PBE. As seen in Table 1, calculations with (PBE+U+vdW) difference to experiment is only 0.23% for lattice constant and 1.0% for bulk modulus. Pressure derivative of the bulk modulus is mostly 4 in solids but all calculations give this value around 5.2 or more. The obtained values with both Hubbard U parameter and van der Waals functional (PBE+U+vdW) (a_0=5.559 Å for lattice constant and B_0=47.46 GPa for Bulk modulus) are in excellent agreement with the experimental data.

The calculated results for static dielectric constants and Born effective charges are summarized in Table 2 together with available experimental measurements and some previous calculations. Our calculations are performed from density functional perturbation theory (DFPT) to observe the longitunal and transverse optical phonon splitting (LO-TO) at Γ point. Dielectric constant for all calculations underestimates the experimental value. Using only Hubbard U term (PBE+U) and using both Hubbard U and van der Waals functional (PBE+U+vdW) has a better agreement with the experiment. Implementing Hubbard U and van Der Waals functional to the PBE doesn't have an appreciable effect on Born effective charge calculations. Effective charges of all calculations are almost same, and slightly larger than experiment. As seen in Table 2, dielectric constants and Born effective charges are in good agreement with other calculations. The tend of overestimation of dielectric constant and Born effective charge of AgCl can be attributed to PBE.

Table 2. Lattice Static dielectric constant ε_∞ and Born effective charge Z^*

Study	ε_∞	Z_{Ag}	Z_{Cl}
This Work (PBE)	4.98(25.4%)	1.45(7.4%)	-1.45(7.4%)
This Work (PBE + U)	4.44(11.8%)	1.48(9.6%)	-1.48(9.6%)
This Work (PBE + vdW)	5.09(28.2%)	1.45(7.4%)	-1.45(7.4%)
This Work (PBE + U+vdW)	4.55(14.6%)	1.48(9.6%)	-1.48(9.6%)
Other Calc (GGA-PBE) (Yang et al.,, 2019)	4.94(24.4%)	1.45(7.4%)	-1.45(7.4%)
Other Calc (GGA-PW91) (Benmessabih et al., 2007)	4.91(23.6%)		
Expt.(Falter et al., 1984)	3.97	1.35	-1.35

Phonon properties

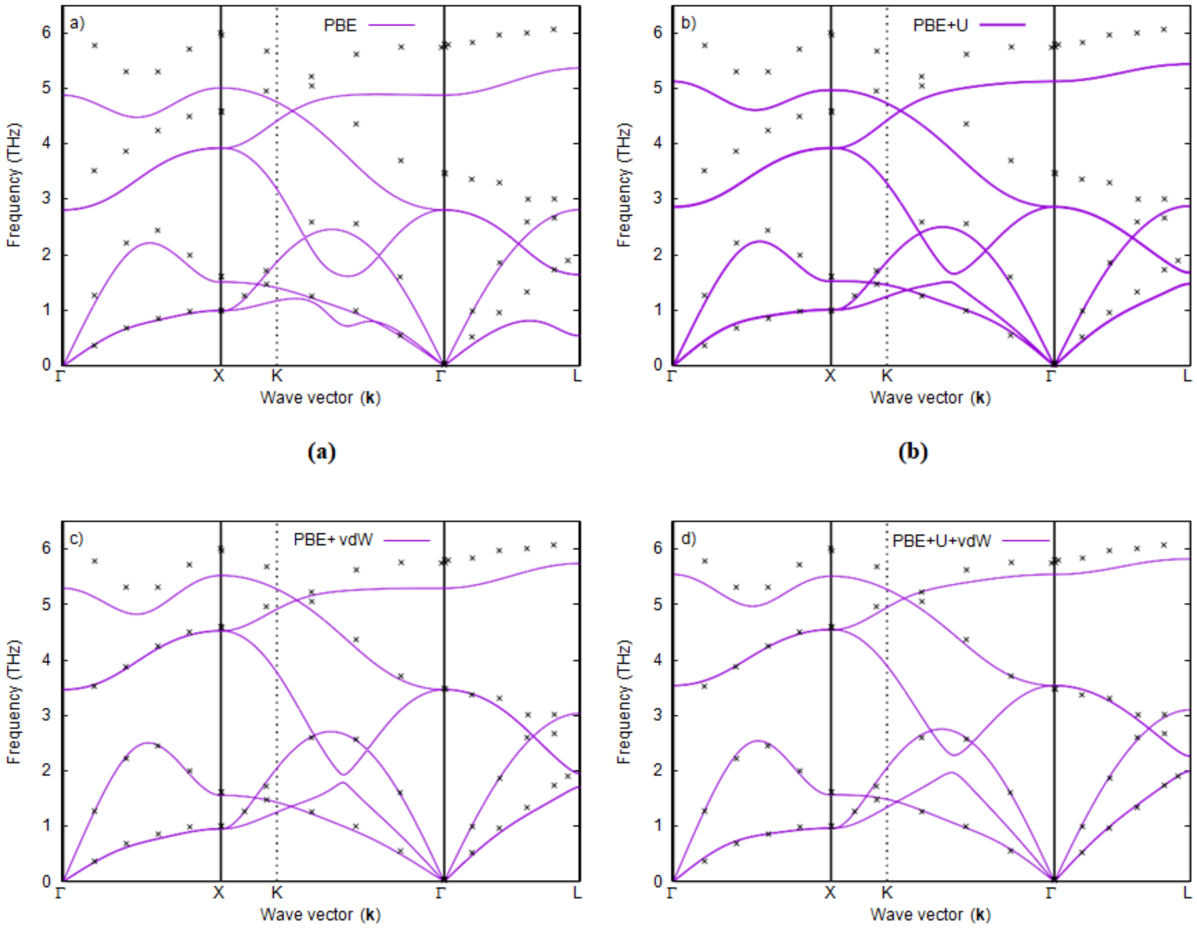

(a) (b)

(c) (d)

Figure 1. Phonon dispersion relations of AgCl along with high symmetry points of the Brillouin zone for a) PBE, b) PBE+U, c) PBE+vdW and d) PBE+U+vdW. Experimental results (cross dots) are taken from neutron neutron scattering measurements of (Vijayaraghavan et al., 1970)

Phonon dispersion relations of AgCl crystal for PBE, PBE+U, PBE+vdW and PBE+U+vdW are presented in Fig. 1 along high symmetry directions Γ-*X*-*K*-Γ-*L* of Brillouin zone. The absence of imaginary (negative frequencies in the figures) phonon frequencies in phonon dispersion curve, give an indication that the AgCl crystal in rock-salt structure is dynamically stable. There exists six phonon modes in the phonon spectrum; two of them transverse acoustic modes (TA), one of them longitudinal acoustic mode (LA), two of them transverse optic modes (TO), and one of them longitudinal optic mode (LO). For all graphs, experimental dispersion relations are taken from the neutron scattering study of (Vijayaraghavan et al., 1970).

The phonon spectrum calculated with pure PBE is given in Figure 1 (a) together with the experimental data. Unlike experiment, PBE leads to softenings on phonon branches in Γ-*L* and *X*-Γ directions. Addition, PBE largely underestimates the optical mode phonon frequencies for nearly every direction. The results are in agreement closely with the earlier calculations (Li et al., 2006; Yang et al., 2019; Gordienko et al., 2010). It is evident that pure PBE does not quite satisfactory present both optical and acoustic phonon modes at all directions for AgCl rock-salt structure.

The Hubbard U implemented PBE+U calculations are reported in Figure 1 (b) As can be seen in the figure, the softenings of PBE in the Γ-*L* and *X*-Γ directions are partially disappeared in PBE+U. Although PBE+U acoustic modes show better agreement with experimental results, the underestimation of high optical modes still exists PBE+U.

As shown in PBE+vdW calculations (Figure 1 (c)), adding van der Waals functional to PBE clearly improved the agreement in both acoustic and optical modes phonon branches except lowest branch in Γ-*L* direction where the acoustic modes are still not consistent with experiment. Finally, as shown in Figure 1 (d), when Hubbard U and van der Waals functional together applied to PBE, the calculated Γ-*L* direction acoustic mode phonon frequencies perfectly describe the experiment.

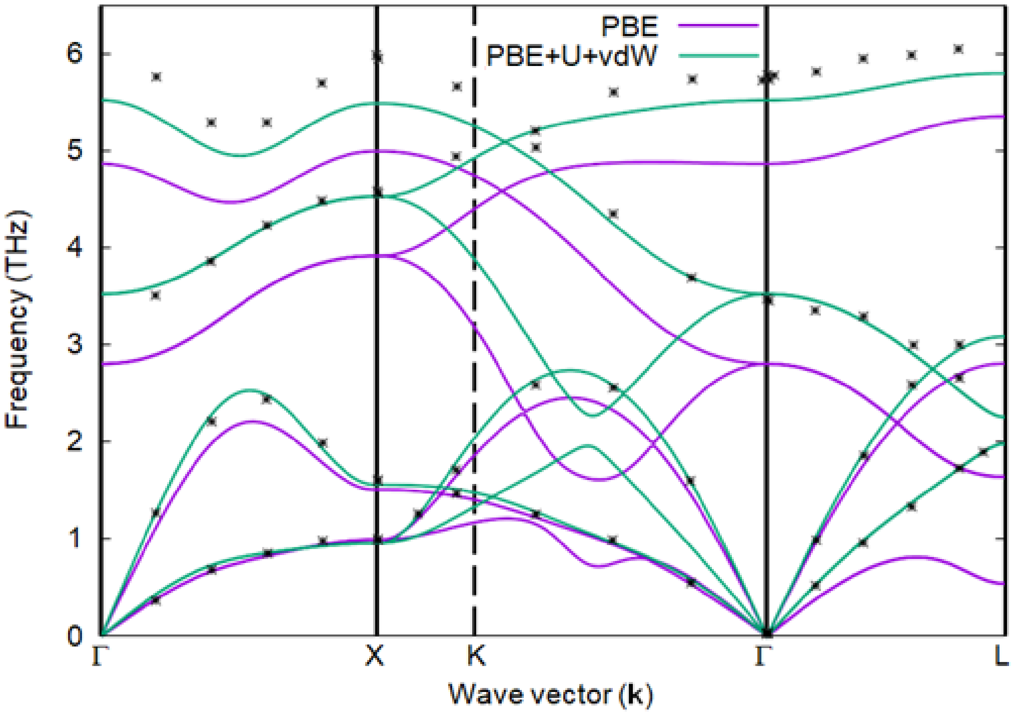

Figure 2. Phonon dispersion relations of AgCl along with high symmetry points of the Brillouin zone

Figure 2 shows the difference between pure PBE and PBE+U+vdW. It is clear that PBE+U+vdW greatly improves the phonon dispersion relations. There is an excellent agreement on all acoustic modes and TO optic modes. For LO modes, the average underestimation of PBE calculations compared to experiment is about 15%. By applying vdW interations and Hubbard U correction, the average underestimation is only 5%.

CONCLUSION

To summarize, the study of the structural, dielectric, and lattice dynamical properties of AgCl rock-salt structure have performed using density functional theory and generalized gradient approximation with PBE parametrization. The calculations have been carried out with and without or both Hubbard U term and van der Waals functional to consider the effect of correlation effects and long range van der Waals bonds, respectively.

PBE calculations for the equilibrium lattice constant, bulk modulus, and its pressure derivative agree nicely with earlier reported works in literature and as in general overestimate experiments and optical phonon modes underestimate experimental results. Taking into account Hubbard U term and van der Waals functional leads to a significant improvement in structural parameters and phonon frequencies, thus beter agreement with experimental results.

The calculated equilibrium lattice constant and Bulk modulus with both Hubbard U term and van der Waals functional overestimate experiments only 0.23% and 1% respectively. For dielectric constant, calculations with Hubbard U (PBE+U) and both Hubbard U and van der Waals functional (PBE+U+vdW) improved the results and leads good agreement with experimental value. Including Hubbard U and/or van der Waals functional is found to be ineffective for Born effective charges.

It is clear that, the pure PBE is not sufficient to describe phonon dispersions. Applying Hubbard U term to PBE (PBE+U) does not make a contribution to improving the optical modes, hovewer adding van der Waals functional (PBE+vdW) has an exact estimation of both acoustic modes and optical modes and greatly improved them. On the other hand, lowest Γ-L acoustic mode still perfectly does not describes experiment. And finally, the best agreement with experimental data was achieved by applying both Hubbard U and van der Waals functional together to PBE (PBE+U+vdW). There is an excellent agreement on all acoustic modes and TO optic modes. For LO modes, the average underestimation is only 5%.

This study ultimately illustrate the necessity of the Hubbard U and van der Waals functional correction on accurate prediction of physical properties of AgCl rock-salt structure.

REFERENCES

Ahn D, Park S, 2016. Cuprous halides semiconductors as a new means for highly efficient light-emitting diodes. Scientific Reports 6: 1-9.

Amrani B, Ahmed R, El Haj Hassan F, Reshak A, 2008. Structural, electronic and optical properties of AgI under pressure. Physics Letters A 372(14): 2502-2508.

An C, Wang S, Sun Y, Zhang Q, Zhang J, Wang C, Fang J, 2016. Plasmonic silver incor- porated silver halides for efficient photocatalysis. Journal of Materials Chemistry A 4(12): 4336-4352.

Anisimov V, Zaanen J, Andersen O, 1991. Band theory and Mott insulators: Hubbard U instead of Stoner I. Physical Review B 44(3): 943-954.

Assis M, et al., 2020. Ag Nanoparticles/AgX (X=Cl, Br and I) Composites with Enhanced Photocatalytic Activity and Low Toxicological Effects. ChemistrySelect, 5: 4655–4673.

Baroni S, Gironcoli S, Dal Corso A, 2001. Giannozzi P. Phonons and related crystal properties from density-functional perturbation theory. Reviews of Modern Physics 73(2): 515-562.

Becquerel A, 1839. Recherches sur les effets de la radiation chimique de la lumiere solaire au moyen des courants electriques, CR Acad. Sci 9(145): 561.

Benmessabih T, Amrani B, 2007. El Haj Hassan F, Hamdache F, Zoaeter M. Computational study of AgCl and AgBr semiconductors. Physica B: Condensed Matter 392(1-2): 309-317.

Cha J, Jung D, 2017. Air-Stable Transparent Silver Iodide-Copper Iodide Heterojunction Diode. ACS Applied Materials and Interfaces 9(50): 43807-43813.

Choudhary et al., 2018. Data Descriptor: Computational screening of high-performance optoelectronic materials using OptB88vdW and TB-mBJ formalisms. Scientific Data 5: 180082.

Consiglio A, Tian Z, 2016. Importance of the Hubbard correction on the thermal conductivity calculation of strongly correlated materials: A case study of ZnO. Scientific Reports 6: 36875.

Falter C, Ludwig W, Selmke M, Zierau W, 1984. An alternative definition of ionicity on a microscopic scale. Physics Letters A 105(3): 139-144.

Faustino M, et al., 2018. CuI p-type thin films for highly transparent thermoelectric p-n modules. Scientific Reports 8(1): 6867-6877.

Gao W, Xia W, Wu Y, Ren W, Gao X, Zhang P, 2018. Quasiparticle band structures of CuCl, CuBr, AgCl, and AgBr: The extreme case. Physical Review B 98(4): 1-10.

Giannozzi P, et al., 2009. QUANTUM ESPRESSO: a modular and open-source software project for quantum simula- tions of materials. Journal of Physics: Condensed Matter 21(39): 395502.

Giannozzi P, et al., 2017. Advanced capabilities for materials modelling with Quantum ESPRESSO. Journal of Physics: Condensed Matter 29: 465901.

Gordienko A, Kravchenko N, Sedelnikov A, 2010. Ab initio calculations of the lattice dynamics of silver halides. Russian Physics Journal 53(7): 692-697.

Grundmann M, Schein F, Lorenz M, Bontgen T, Lenzner J, Wenckstern von H, 2013. Cuprous iodide: A p-type transparent semiconductor, history, and novel applications. Physica status solidi A 210(9): 1-33.

Hebbache M, Zemzemi M, 2004. Ab initio study of high-pressure behavior of a low compressibility metal and a hard material: Osmium and diamond. Physical Review B Condensed Matter and Materials Physics 70(22): 5-10.

Hull S, Keen D, 1999. Pressure-induced phase transitions in AgCl, AgBr, and AgI. Physical Review B 59(2): 750-761.

Jiang H, 2018. Revisiting the GW approach to d - And f -electron oxides. Physical Review B 97(24): 1-9.

Jossou E, Malakkal L, Szpunar B, Oladimeji D, Szpunar J, 2017. A first principles study of the electronic structure, elastic and thermal properties of UB2. Journal of Nuclear Materials 490: 41-48.

Kirchhoff F, Holender J, Gillan M, 1994. Energetics and electronic structure of silver chloride. Physical Review B 49(24):17420-17423.

Klimes J, Bowler D, Michaelides A, 2010. Chemical accuracy for the van der Waals density functional. Journal of Physics: Condensed Matter 22(2): 022201.

Li Y, Zhang L J, Cui T, Li Y W, Wang Y, Ma Y M, Zou G T, 2008. First-principles studies of phonon instabilities in AgI under high pressure. Journal of Physics: Condensed Matter 20(19): 195218.

Li Y, Zhang L, Cui T, Ma Y, Zou G, Klug D, 2006. Phonon instabilities in rocksalt AgCl and AgBr under pressure studied within density functional theory. Physical Review B 74(5): 054102.

Masumoto Y, Wamura T, Iwaki A, 1989. Homogeneous width of exciton absorption spectra in CuCl microcrystals. Applied Physics Letters 55(24): 2535-2537.

Mellander B E, 1982. Electrical conductivity and activation volume of the solid electrolyte phase AgI and the high-pressure phase fcc AgI. Physical Review B 26(10): 5886-5896.

Mellander B E, Lunden A, Friesel M, 1981. High pressure studies of silver iodide and copper iodide. Solid State Ionics 5(C): 477-479.

Mukhopadhyay S, Bansal D, Delaire O, Perrodin D, Bourret-Courchesne D, Singh D J, Lindsay L, 2017. The curious case of cuprous chloride: Giant thermal resistance and anharmonic quasiparticle spectra driven by dispersion nesting. Physical Review B 96(10): 100301.

Nunes G S, Allen P B, Martins J L, 1998. Pressure-induced phase transitions in silver halides. Physical Review B 57(9): 5098-5105.

Okoye C, 2004. Investigation of the pressure dependence of band gaps for silver halides within a first-principles method. Solid State Communications 129(1): 69-73.

Palomino-Rojas L, L´opez-Fuentes M, Cocoletzi G, Murrieta G, Coss R, Takeuchi N, 2008. Density functional study of the structural properties of silver halides: LDA vs GGA calculations. Solid State Sciences 10(9): 1228-1235.

Patnaik J, Sunandana C, 1998. Studies on gamma silver iodide. Journal of Physics and Chemistry of Solids 3697(97): 1059-1069.

Perdew J, Burke K, Ernzerhof M, 1996. Generalized Gradient Approximation Made Simple. Physical Review Letters 77(18): 3865-3868.

Saito K, Hasuo M, Hatano T, Nagasawa N, 1995. Band gap energy and binding energies of Z3-excitions in CuCl. Solid State Communications 94(1): 33-35.

Smith P, 1976. A tight-binding approach to the electronic structure of the silver halides. Journal of Physics and Chemistry of Solids 37(6): 581-587.

Tejeda J, Braun W, Goldmann A, Cardona M, 1974. Valence bands of silver halides de- termined by X-ray and UV photoemission. Journal of Electron Spectroscopy and Related Phenomena 5(1): 583-592.

Tejeda J, Shevchik N, Braun W, Goldmann A, Cardona M, 1975. Valence bands of AgCl and AgBr: Uv photoemission and theory. Physical Review B 12(4): 1557-1566.

Tolba S, Gameel K, Ali B, Almossalami H, Allam N, 2018. The DFT+U: Approaches, Accuracy, and Applications. Density Functional Calculations-Recent Progresses of Theory and Application (InTech) pp.3-30. DOI: https://doi.org/10.5772/intechopen.72020

Vanderbilt D, 1990. Soft self-consistent pseudopotentials in a generalized eigenvalue formalism. Physical Review B 41(11): 7892-7895.

Vijayaraghavan P, Nicklow R, Smith H, Wilkinson M, 1970. Lattice Dynamics of Silver Chloride. Physical Review B 1(12): 4819-4826.

Victora R, 1997. Calculated electronic structure of silver halide crystals. Physical Review B 56(8): 4417-4421.

Vogel D, Kruger P, Pollmann J, 1998. Ab initio electronic structure of silver halides calculated with self-interaction and relaxation-corrected pseudopotentials. Physical Review B - Condensed Matter and Materials Physics 58(7): 3865-3869.

Wang Y, Ye C, Wang G, Zhang L, Liu Y, Zhao Z, 2003. In situ x-ray diffraction study on AgI nanowire arrays. Applied Physics Letters 82(24): 4253-4255.

Yang C, et al, 2017. Transparent flexible thermoelectric material based on non-toxic earth-abundant p-type copper iodide thin film. Nature Communications 8: 16076.

Yang X, Dai Z, Zhao Y, Meng S, 2019. Superhigh thermoelectric figure of merit in silver halides AgCl and AgBr from first principles. arXiv:1904.06010.

Zhang G, Tkatchenko A, Paier J, Appel H, Scheffler M, 2011. van der Waals Interactions in Ionic and Semiconductor Solids. Physical Review Letters 107(24): 245501.

Zhang M, Jiang H, 2019. Electronic band structure of cuprous and silver halides: An all- electron GW study. Physical Review B 100(20): 205123.

Zhu H, Liu A, Noh Y, 2019. Transparent Inorganic Copper Bromide (CuBr) p-Channel Transistors Synthesized From Solution at Room Temperature. IEEE Electron Device Letters 40(5): 769-772.